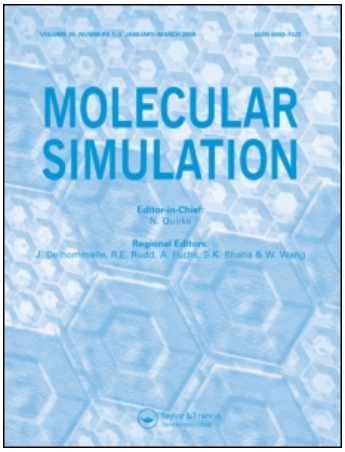

Molecular Simulation
Publication details, including instructions for authors and subscription information:
http://www.informaworld.com/smpp/title~content=t713644482

Constant surface tension molecular dynamics simulations of lipid bilayers with trehalose

R. M. Venable[a]; A. Skibinsky[a]; R. W. Pastor[a]
[a] Laboratory of Biophysics, Center for Biologics Evaluation and Research, FDA, Rockville, MD, USA

To cite this Article Venable, R. M. , Skibinsky, A. and Pastor, R. W.(2006) 'Constant surface tension molecular dynamics simulations of lipid bilayers with trehalose', Molecular Simulation, 32: 10, 849 — 855
To link to this Article: DOI: 10.1080/08927020600615018
URL: http://dx.doi.org/10.1080/08927020600615018

Molecular Simulation, Vol. 32, Nos. 10–11, 30 August–15 September 2006, 849–855

Taylor & Francis
Taylor & Francis Group

Constant surface tension molecular dynamics simulations of lipid bilayers with trehalose

R. M. VENABLE, A. SKIBINSKY and R. W. PASTOR*

Laboratory of Biophysics, Center for Biologics Evaluation and Research, FDA, 1401 Rockville Pike, Rockville, MD 20852-1448, USA

(Received February 2006; in final form February 2006)

Surface areas and fluctuations evaluated from 50 ns molecular dynamics simulations of fully hydrated dipalmitoylphosphatidylcholine (DPPC) bilayers in a 1:2 trehalose:lipid ratio carried out at surface tensions 10, 17 and 25 dyn/cm/leaflet are compared with those of pure bilayers under the same conditions. Trehalose increases the surface area, as consistent with the surface tension lowering observed in simulations at constant area. The system bulk elastic modulus $K_b = 1.5 \pm 0.3 \times 10^{10}$ dyn/cm^2. It is independent of bilayer surface area and trehalose content within statistical error. In contrast, the area elastic modulus K_a shows a strong area dependence. At 64 Å^2/lipid (the experimental surface area), $K_a = 138 \pm 26$ dyn/cm for a pure DPPC bilayer and 82 ± 10 dyn/cm for one with trehalose; i.e. trehalose increases fluidity of the bilayer surface at this area per lipid.

Keywords: DPPC; Isotherm; Equivalence of ensembles; Area compressibility modulus; Bulk compressibility modulus

1. Introduction

This paper primarily concerns the effect of trehalose on surface area and volume fluctuations of fluid phase lipid bilayers, and the related quantities K_a (the surface area elastic modulus) and K_b (the bulk elastic modulus). Trehalose (figure 1) is a highly effective preservative of cells and liposomes [1,2], and its effect on bilayer elasticity or fluidity may yield insight into its mechanism of action [2]. We build upon recently published [3] molecular dynamics (MD) simulations of fully hydrated dipalmitoylphosphatidylcholine (DPPC) bilayers in a 1:2 trehalose:lipid ratio. These systems were simulated at a range of surface areas at NPAT (constant number N, normal pressure P, area A, and temperature T) and surface tension at NPγT (γ is the applied surface tension). The trajectories of 20–25 ns each were sufficiently long to develop surface tension-surface area isotherms that could fruitfully be compared between ensembles, with those of pure DPPC bilayers, and with monolayers. This study extends the six constant surface tension trajectories to 50 ns, a length more suitable for evaluating the volume and area fluctuations, and thereby the elastic moduli. The availability of these quantities also allows a test of the accuracy of the potential energy parameters for pure systems, and a discussion of related results from other recent simulations of pure bilayers [4–7] and those with added trehalose [8–10].

2. Methods

The construction and simulation of the trehalose/bilayer systems at 323.15 K are detailed in reference 3. Briefly, the bilayers consisted of 80 lipids (40/leaflet) and were fully hydrated (20–29 waters/lipid); those with sugars contained 40 trehalose. NPγT trajectories were extended from 20 ($\gamma = 10$ dyn/cm/leaflet) or 25 ns ($\gamma = 17$ and 25 dyn/cm/leaflet) to 50 ns for all six systems (table 1). The pure DPPC NPγT systems contained 2324 waters, and those with trehalose contained 1629. The simulation times of the NPAT trehalose/bilayer systems and the pure bilayer at $A = 64$ Å^2/lipid were extended from 20 to 25 ns (see table 2 for a complete listing of surface areas and trajectory lengths). The experimentally determined surface area of DPPC bilayers under these conditions is 64 Å^2/lipid [11].

Results for the following three simulations are also discussed: 1340 waters (12.5 ns at NPT); 1629 waters with 40 trehalose (20 ns at NPAT, the same numbers of water

*Corresponding author. Email: richard.pastor@fda.hhs.gov

Molecular Simulation
ISSN 0892-7022 print/ISSN 1029-0435 online © 2006 Taylor & Francis
http://www.tandf.co.uk/journals
DOI: 10.1080/08927020600615018

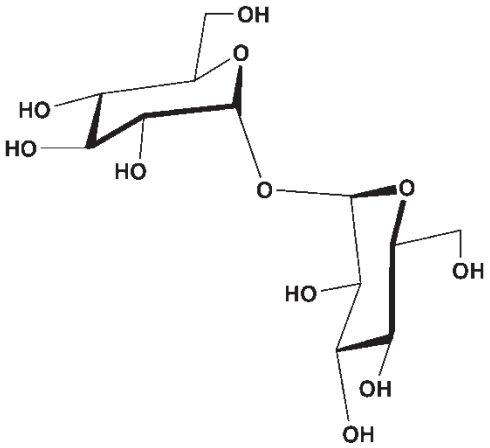

Figure 1. α,α-Trehalose (1,1-α-D-Glucopyranosyl α-D-glucopyranoside). Henceforth, this disaccharide is simply denoted trehalose.

and trehalose as the bilayers simulated at NPγT); and 1117 waters with 80 trehalose (25 ns at NPAT). The preceding two trehalose solutions are 1.363 and 3.976 molal, respectively.

Simulations were carried out using CHARMM (Chemistry at HARvard Macromolecular Mechanics) [12] with the C27r all-atom potential energy set for DPPC [13], CSFF for trehalose [14] and modified TIP3P for water [15,16], a 1-fs time step, and tetragonal periodic boundary conditions. Temperatures and pressures were maintained by extended system methods [17,18] and electrostatic interactions were calculated using particle mesh Ewald [19]. Lennard-Jones energies were switched to zero between 7 and 10 Å. Because lipid monolayers were simulated at constant volume in the original study, the recently developed [20] pressure-based long range correction (LRC) was not included in any of the simulations presented here. This is expected to have a small effect of the calculated surface tensions of the bilayers [20]. However, neglect of the LRC leads to overestimates of the isothermal compressibility for neat fluids [13,20], and one purpose of this study is to determine the importance of this correction for area compressibility of bilayers.

Table 1. Total densities ρ, surface area per lipid A, bulk compressibilities K_b, and area compressibilities K_a for pure DPPC bilayer systems and those with 40 trehalose (+ treh) simulated at NPγT. Standard errors for ρ are <0.001 gm/cm^3; those for other quantities are in parentheses. K_b and K_a were evaluated from volume and area fluctuations, respectively. All trajectories were 50 ns.

γ(dyn/cm)	ρ(g/cm^3)	A(Å^2)	K_b(10^{10} dyn/cm^2)	K_a(dyn/cm)
10 pure	0.993	59.9 (0.2)	1.3 (0.2)	320 (89)
+ treh	1.025	60.8 (0.6)	1.5 (0.2)	180 (36)
17 pure	0.990	67.6 (0.6)	1.5 (0.4)	93 (25)
+ treh	1.020	72.0 (0.9)	1.5 (0.3)	83 (25)
25 pure	0.986	81.1 (0.7)	1.4 (0.1)	85 (24)
+ treh	1.018	89.9 (1.5)	1.5 (0.4)	55 (18)

Table 2. Trajectory lengths, total densities ρ, surface tensions A, and bulk compressibilities K_b (from volume fluctuations) for pure DPPC bilayer systems and those with 40 trehalose (+ treh) simulated at NPAT. Standard errors for ρ are <0.001 gm/cm^3; those for other quantities are in parentheses.

Area (Å^2)	Time (ns)	ρ(g/cm^3)	γ(dyn/cm)	K_b(10^{10} dyn/cm^2)
54 pure	20	0.999	1.2 (1.4)	1.7 (0.5)
+ treh	25	1.043	−4.2 (1.9)	1.9 (1.1)
60 pure	15	0.993	9.4 (1.2)	1.6 (1.3)
64 pure	25	0.990	16.8 (1.0)	1.5 (0.3)
+ treh	25	1.035	11.2 (1.2)	1.7 (0.5)
68 pure	15	0.989	19.2 (0.8)	1.5 (0.3)
80 pure	20	0.987	23.9 (0.5)	1.5 (0.2)
+ treh	25	1.030	19.7 (1.3)	1.4 (0.4)

Surface tensions were evaluated from the relation [21,22]:

$$\gamma = \frac{1}{2}\left\langle L_z\left(P_{zz} - \frac{1}{2}(P_{xx} + P_{yy})\right)\right\rangle \tag{1}$$

where L_z is the length of the simulation cell normal to the bilayer surface, P_{zz} is the component of the pressure tensor normal the bilayer surface, and P_{xx} and P_{yy} are the tangential components. The factor of 1/2 arises because there are two interfaces in the system, so the units of surface tensions reported here are understood to be dyn/cm/leaflet; units for applied surface tension are omitted when the context is clear.

The bulk modulus was evaluated from the average volume $\langle V\rangle$ and its fluctuations $\langle \delta V^2\rangle$ as follows

$$K_b = -V\left(\frac{\mathrm{d}P}{\mathrm{d}V}\right)_T = \frac{k_B T\langle V\rangle}{\langle \delta V^2\rangle} \tag{2}$$

where k_B is Boltzmann's constant. K_b is the inverse of the isothermal compressibility β_T. The area compressibility modulus was obtained from both the derivative relation and the average total area and its fluctuations:

$$K_a = A\left(\frac{2\mathrm{d}\gamma}{\mathrm{d}A}\right)_T = \frac{k_B T\langle A_{\mathrm{tot}}\rangle}{\langle \delta A_{\mathrm{tot}}^2\rangle}. \tag{3}$$

Equation 3 here differs from equation 3 of reference 23, where surface areas and fluctuations were evaluated on a per lipid basis.

Fluctuations in spatial dimensions in simulations carried out with the extended system method used here are independent of the piston mass. In contrast, simulations carried out with the weak-coupling algorithm [24] may show dependence on the coupling constant [25], and require further validation when evaluating K_b and K_a [4].

When evaluating averages for the pure bilayers, the first 3 and 5 ns were deleted from NPAT and NPγT trajectories, respectively. For systems with trehalose, averaging began at 10 ns for NPAT simulations and NPγT simulations at $\gamma = 10$ and 17, and at 15 ns for $\gamma = 25$.

3. Results and discussion

3.1 γ-A isotherm

Figure 2 plots the area time series for the six constant surface tension trajectories. The equilibration time of 10–15 ns for the systems with trehalose is dictated by the time scale of intercalation into the headgroup [3]. This intercalation, as well as a substantial fraction of trehalose in solution, is clear from figure 3. Figure 4 plots average surface areas from the preceding trajectories, and the average surface tensions for the constant area simulations (these values differ slightly from those in reference 3 because of additional data). Surface tensions increase with surface area, and points from the two ensembles lie on the same isotherms, indicating that the ensembles are equivalent for the present systems. The increase in surface area upon addition of trehalose relative to the pure systems evident in figure 2 is also consistent with the isotherms. Trehalose lowers the surface tension for systems simulated at NPAT (table 2) and $(\partial\gamma/\partial A)_T > 0$, so the surface area increases until the internal surface tension of the bilayer equals the applied surface tension.

The pure bilayer isotherm is qualitatively similar to those recently reported by Chadresekhar *et al.* [5] based on the GROMOS96 45A3 force field, including the non-zero surface tension near the experimental surface area of 64 Å^2/lipid. The GROMOS isotherm is somewhat steeper than in figure 4. From equation 3, this implies a larger surface area compressibility modulus. Isotherms for glycerolmonoolein (GMO) evaluated by Marrink and Mark [6] using the GROMACS force field yielded a similar dependence, but with γ near zero at the area argued to be that of a flaccid bilayer.

The area expansion generated upon the addition of trehalose implies that the thickness of the bilayer must decrease. Membrane thinning has indeed been experimentally observed under these conditions [26].

3.2 Density

As evident from tables 1 and 2, the densities decrease slightly with decreasing area. This is because chain order increases and lipid packing is enhanced. From the density of pure TIP3P water simulated under these conditions (table 3), the volume of unperturbed water $V_{wat} = 30.401$ Å^3. The volume per lipid (V_{lipid}), can then be evaluated from the total volume of the system (V_{tot}), V_{wat}, and numbers of each

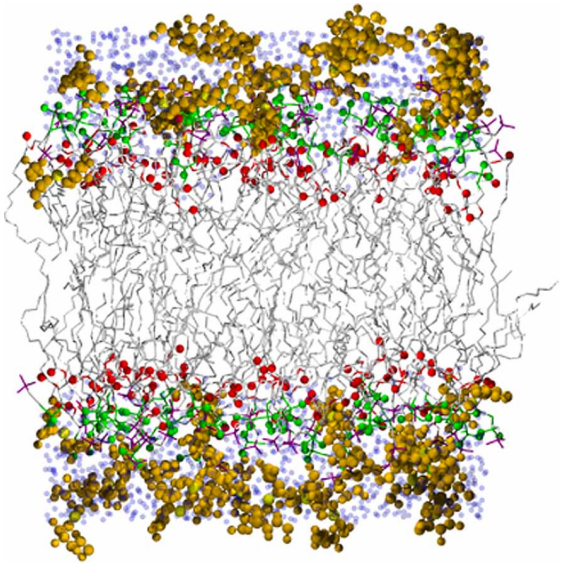

Figure 3. DPPC bilayer with 40 trehalose from the 50 ns point of NPγT simulation at $\gamma = 17$ dyn/cm. Coloring is as follows in online version: glycosidic oxygen of trehalose, yellow; all other trehalose atoms, orange; phosphate groups of DPPC, green; $N(CH_3)_3$, purple; carbonyl oxygen, red; all other lipid atoms, grey; waters, transparent blue. See online version for colour.

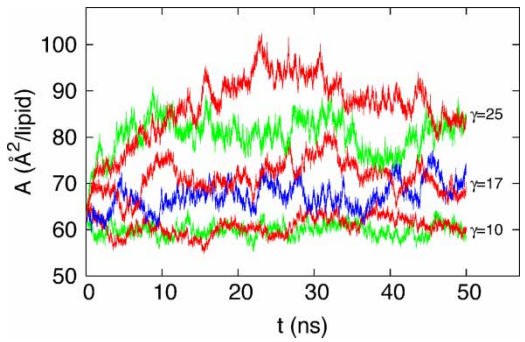

Figure 2. Trajectories of NPγT simulations of pure bilayers (blue for $\gamma = 17$ dyn/cm; green for $\gamma = 10$ and 25 dyn/cm) and bilayers with trehalose (red) in online version.

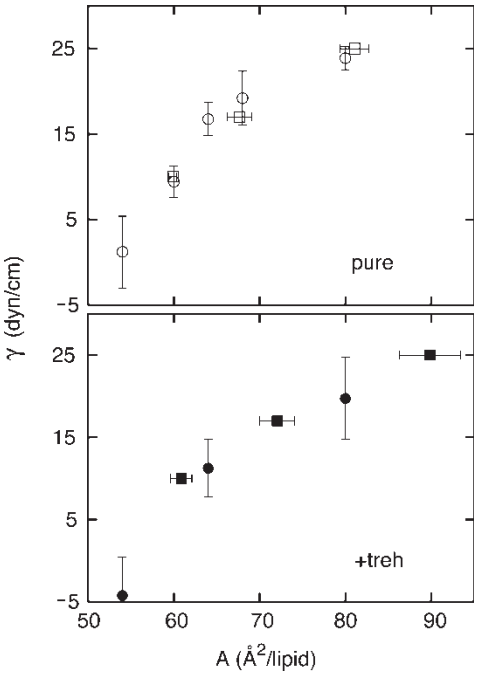

Figure 4. Surface tension-surface area isotherms at 323 K for pure DPPC (top, open symbols) and DPPC with 40 trehalose (bottom, filled symbols). Simulations carried out at NPAT in circles; those at NPγT in squares. Error bars specify the 95% confidence intervals.

Table 3. Simulated densities and bulk compressibilities (from volume fluctuations) for trehalose solutions with molalities of 0 (pure water), 1.363 (40 trehalose and 1629 water, the same as contained in the NPγT lipid/water/trehalose systems), and 3.976 (80 trehalose and 1127 water). Standard errors are in parentheses. Experimental densities are from reference 27 for water and reference 28 for trehalose solutions.

Treh molality	ρ *(g/cm^3)*	ρ *(g/cm^3) (exp)*	K_b *(10^{10} dyn/cm^2)*
0	0.9834	0.9881	1.68 (0.05)
1.363	1.0964 (0.0003)	1.126 (0.001)	2.03 (0.04)
3.796	1.2060 (0.0002)	1.261 (0.005)	2.65 (0.04)

component [29]:

$$V_{\text{tot}} = n_{\text{wat}} \times V_{\text{wat}} + n_{\text{lipid}} \times V_{\text{lipid}}. \quad (4)$$

For $\gamma = 17$ dyn/cm, $V_{\text{tot}} = 168{,}752 \pm 78$ Å^3, yielding $V_{\text{lipid}} = 1226 \pm 1$ Å^3. For the constant area simulation at 64 Å^2/lipid, $V_{\text{lipid}} = 1225 \pm 1$ Å^3. These compare very favorably with the experimental value of 1232 Å^3 [11].

The density increases of 11.5 and 22.6% for 1.363 and 3.796 molal trehalose relative to pure water compare well with the experimentally observed increases of 14.0 and 26.6% (table 3). This agreement lends further support to the accuracy of the carbohydrate/water interaction parameters.

Upon addition of trehalose the system densities increase by approximately 3% for each surface tension (table 1) and 4% for each surface area (table 2). This change mostly arises from the increased density of the solution phase. Specifically, from the preceding estimate of V_{lipid}, the volume fraction of water is approximately 0.4. If mixing were ideal, 40% of the system would be expected to increase in density by 11.5% (table 3), for a overall density increase of 4.6%. Increases in the surface area (which lowers bilayer density) and intercalation of trehalose into the headgroup region (which lowers the concentration of trehalose in the water region but increases the bilayer density) lead to slightly smaller observed values.

3.3 Bulk elastic modulus

From table 1, the K_b are independent of the surface area. The simulated bulk elastic modulus for trehalose/water solution is 20% higher than that of pure water (table 3), but the effects of this difference are not discernable within the relatively large statistical uncertainty of the K_b for the bilayer/water systems. The bulk compressibilities from the NPAT simulations are comparable to those at NPγT, though the statistical errors are larger because of the shorter length of the trajectories (table 2).

The bulk elastic modulus for the bilayer alone may be estimated from

$$K_b = f_{\text{wat}} \times K_b(\text{water}) + (1 - f_{\text{wat}}) \times K_b(\text{bilayer}) \quad (5)$$

where f_{wat} is the volume fraction of water. For $\gamma = 17$ dyn/cm, $f_{\text{wat}} = 0.416$ and $K_b(\text{bilayer}) = 1.3 \pm 0.3 \times 10^{10}$ dyn/cm^2. This is 40% below the experimental value of 2.1×10^{10} dyn/cm^2 for pure DPPC bilayers [30]. The discrepancy between simulation and experiment can most likely be attributed to the neglect of the LRC. Simulations [20] of pentadecane at 312 K using the CHARMM parameter set C27 yielded $K_b = 1.05$ (with LRC) and 0.78 (no LRC), as compared to the experimental value of 1.09×10^{10} dyn/cm^2 [26]. Hence, the parameter set underestimates K_b by 27% when the LRC is not included. Likewise, the simulation of water carried out here without the LRC (table 3), underestimates the experimental value of 2.27×10^{10} dyn/cm^2 [27] by 26%. Including the LRC substantially reduces the error for both alkanes and water [20], and it is reasonable to propose that this correction will yield similar good agreement for bilayers.

Equation 5 can be written for bilayer/trehalose systems as follows

$$K_b = f_{\text{sol}} \times K_b\,(\text{solution}) + (1 - f_{\text{sol}}) \times K_b(\text{bilayer} + \text{trehalose}) \quad (6)$$

where f_{sol} is the fraction of trehalose/water solution. Setting $f_{\text{sol}} = 0.4$ (as in the preceding density calculations) and $K_b\,(\text{solution}) = 2.03 \times 10^{10}$ dyn/cm^2 (table 3) yields $K_b\,(\text{bilayer} + \text{trehalose}) = 1.1 \times 10^{10}$ dyn/cm^2. This is approximately 15% lower than $K_b\,(\text{bilayer})$ estimated above. However, it is within the 20–30% statistical error in K_b from the simulations, so it is most reasonable to infer that trehalose leaves $K_b\,(\text{bilayer})$ unchanged.

3.4 Area elastic modulus

K_a evaluated from the area fluctuations are listed in table 1 and plotted in figure 5. While the fluctuations in surface area per lipid evident in figure 2 lead to substantial statistical errors, it is clear that systems at low areas are substantially stiffer than at high areas. Note from figure 4 that isotherms are approximately parallel, steep at low areas and relatively flat at high areas. Consequently, bilayers at high surface area are more sensitive to changes in the surface tension. This explains why the addition of trehalose dramatically expands the bilayer at $\gamma = 25$, but has little effect $\gamma = 10$.

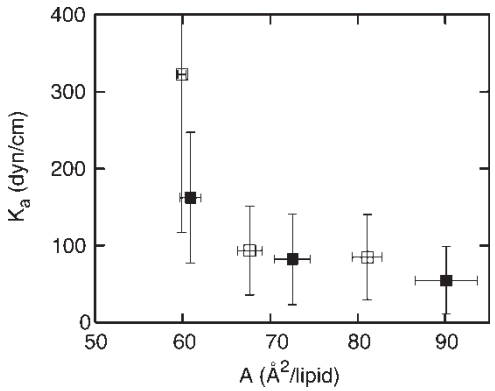

Figure 5. Area elastic modulus vs. area from NPγT simulations of pure DPPC (open squares) and DPPC with trehalose (filled squares), with 95% confidence intervals in both variables.

A more precise estimate for K_a at a specific area is obtained by combining γ-A values from the constant area and surface tension simulations and using the derivative relationship in equation 3. The slopes of the γ-A isotherms between 59 and 73 Å^2/lipid (figure 6) yield $K_a = 138 \pm 26$ dyn/cm for a pure bilayer at 64 Å^2/lipid and 82 ± 10 dyn/cm for one with trehalose. Hence, at the present low concentration, trehalose makes the bilayer surface somewhat less stiff. This is consistent with the proposal of Crowe *et al.* [2] that trehalose makes cell membranes more fluid. These authors also argue that such fluidity may inhibit phase separation during dehydration and thereby limit dehydration damage.

The preceding value of K_a for pure DPPC is in the experimental range obtained for dimyristoylphosphatidylcholine (DMPC) at a comparable temperature above its main phase transition. Early work by Evans and Rawicz [31] using micropipette aspiration yielded $K_a = 140$ dyn/cm, in close agreement with values obtained by Gawrisch from osmotic pressure [32]. More recently, Rawicz *et al.* [33] argued that the preceding values are associated with eliminating long wavelength undulations; i.e. creating a microscopically smooth surface, but not stretching it. Further aspiration expands the surface area by explicit stretching, and yields $K_a = 234$ dyn/cm, or approximately 40% larger than obtained here. It is likely that simulations with the LRC would yield higher K_a, closer to the more recent experimental value. However, given the sensitivity of K_a to surface area demonstrated in the present simulations (figure 5), there is also the possibility that some of the variation in experimental results arises from slight differences in conditions that lead to differences in the optimal surface areas.

The K_a are substantially smaller than those obtained earlier for DPPC by Feller and Pastor [23] from area fluctuations over the 500–1000 ps interval of NPγT simulations. The disagreement is largely due to incomplete statistical sampling in short trajectories; i.e. the membrane appeared stiffer because larger excursions from the mean value were not sampled. However, a linear fit to the γ-A isotherm (excluding $\gamma = 0$) from the NPγT data yielded results comparable with the present values, though with a higher statistical uncertainty. More recently, the modulus λ was evaluated for DMPC by nonequilibrium MD [7]. Cycles of compression from the equilibrium state yielded $\lambda = (16.5 \pm 2) \times 10^7$ N/m^2, while expansion cycles yielded $\lambda = (5.3 \pm 2) \times 10^7$ N/m^2. From $K_a = \lambda d$, where the membrane thickness d was assumed to be 34 Å for DMPC, $K_a = 560$ dyn/cm (from contraction cycles) and 180 dyn/cm (expansion cycles). The value from the expansion cycle is reasonably close to ours for areas near 64 Å^2/lipid of DPPC. The rather high value of K_a from the compression cycle could be associated with the nonlinear γ-A isotherm and the rapidly increasing stiffness of the bilayer as it is contracted. Anézo *et al.* [4] calculated K_a for a bilayer of 128 DPPC using the GROMACS potential and a variety of electrostatic truncation schemes. They obtained values in the 200–850 dyn/cm range; i.e. mostly somewhat higher than experiment and those reported here. Hence, it appears that the GROMACS parameters yield somewhat stiffer bilayers than C27r.

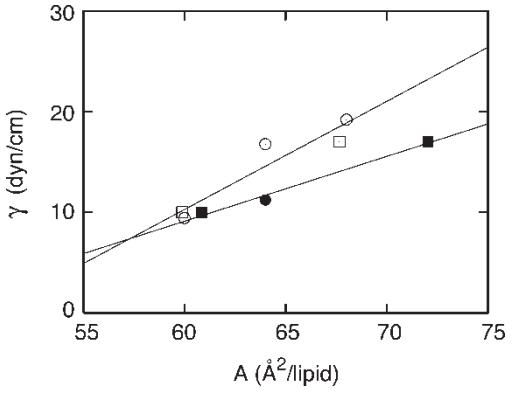

Figure 6. Surface tension-surface area isotherm in the neighborhood of 64 Å^2/lipid with linear fits used to evaluate K_a from $(d\gamma/dA)_T$ (equation 3). Symbols are consistent with those of previous figures: pure DPPC (open); DPPC with trehalose (filled); NPAT (circles); NPγT (squares).

3.5 Comparison with other bilayer/trehalose simulations

Three simulation studies of fully hydrated DPPC bilayers with trehalose have been recently published. Sum, Faller and de Pablo [8] simulated systems of 8 and 27 trehalose with 128 lipids at 350 and 400 K. The systems of Pereira *et al.* [9] were at higher concentrations, 64 and 128 trehalose with 128 lipids, and also at two temperatures, 325 and 475 K. Villarreal *et al.* [10] simulated five systems at 323 K, with the largest consisting of 256 lipids and 72 trehalose. While these authors did not publish values of the elastic moduli, the surface areas and their response to trehalose may be compared with the present results.

The contraction of the pure bilayers to 56 Å^2 at 325 K observed by Pereira *et al.* [9] is consistent with the GROMOS96 45A3 force field. The apparent stabilization of the systems with trehalose is more difficult to explain. It is possible that the parameters used in their study yielded a surface tension near zero when trehalose is added. In this case the system would not contract when simulated at NPT. It is also possible that if the trajectories had been continued past 6 ns a more dramatic contraction would have been observed. Changes in surface area are slow to develop in these systems (figure 2). Their simulations at 475 K showed area expansion for a 1:1 trehalose:lipid ratio. This result appears comparable to those presented here, although the high disorder in the pure system at this temperature makes a more quantitative comparison difficult.

Different force fields can lead to different results. Sum *et al.* [8] used a combination of GROMOS96 and NERD parameters for the lipid, OPLS for the trehalose, and SPC/E for the water. For these parameters, the average surface area of the pure bilayer was close to the experimental value of 64 Å^2/lipid at 325 K when simulated at NPT; i.e. the surface tension is close to zero for the pure

bilayer with these parameters. The addition of trehalose did not change surface area of bilayers heated at 350 and 400 K. The highest ratio of trehalose per lipid in the study is 1:4.7, and it is possible that this is the reason for the negligible expansion. Similar arguments may explain the results of Villarreal *et al.* [10], who also did not observe expansion upon addition of trehalose (though did note a slight reduction in area fluctuations). These authors simulated at NPT with GROMOS-87, a force field that yields the experimentally observed surface area for DPPC under these conditions. Additionally, the concentration 1:3.6 trehalose:lipid ratio is about half of that studied here.

4. Conclusions

Trehalose lowers the surface tensions of DPPC bilayers when the surface area is held constant, and increases the area when the surface tension is held constant. Surface tension-surface area isotherms from NPγT and NPAT simulations are consistent, implying that the two ensembles are equivalent for the present application. This increases the confidence in the study and allows for pooling of data.

The surface elastic modulus strongly depends on area, and is lowered by trehalose at the experimental surface area; i.e. trehalose makes the bilayer surface more fluid. The bulk elastic modulus is, within statistical error, largely insensitive to both surface area and the presence of trehalose.

The results also provide additional support to the CHARMM lipid and carbohydrate potential energy parameters. Bilayer densities, bulk compressibilities and area compressibilities all agree reasonably with experiment, and agreement is expected to be improved by addition of a LRC for the Lennard-Jones interactions. Isotherms for bilayers evaluated for C27r show the same trend of increasing surface tension with increasing surface area as do GROMOS96 45A3 for DPPC and GROMACS for GMO. However, there remain important differences with these and other force fields, such as the slope of the isotherm and the point of zero surface tension. Systematic evaluation of bilayer elastic moduli should prove valuable for comparing and improving force fields.

Acknowledgements

This study utilized the high-performance computational capabilities of the CIT Biowulf/LoBoS3 and NHLBI LOBOS clusters at the National Institutes of Health, Bethesda, MD.

References

[1] W.F. Wolkers, N.J. Walker, Y. Tamari, F. Tablin, H. Crowe. Towards a clinical application of freeze-dried human platelets. *Cell Preservation Technology*, **1**, 175 (2003).

[2] J.M. Crowe, M.A. Whittam, D. Chapman, L.M. Crowe. Interactions of phospholipid monolayers with carbohydrates. *Biochem. Bipohys. Acta*, **769**, 151 (1984).

[3] A. Skibinsky, R.M. Venable, R.W. Pastor. A molecular dynamics study of the response of lipid bilayers and monolayers to trehalose. *Biophys. J.*, **89**, 4111 (2005).

[4] C. Anézo, A.H. de Vries, H.-D. Hö1ltje, D.P. Tieleman, S.J. Marrink. Methodological issues in lipid bilayer simulations. *J. Phys. Chem. B*, **107**, 9424 (2003).

[5] I. Chandrasekhar, A. Glättli, P. Hünenberger, C. Pereira, W.F. van Gunsteren. Molecular dynamics simulations of lipid bilayers with GROMOS96: application of surface tension. *Mol. Sim.*, **31**, 543 (2005).

[6] S.J. Marrink, A.E. Mark. Effect of undulations on surface tension in simulated membranes. *J. Phys. Chem. B*, **105**, 6122 (2001).

[7] G. Ayton, A.M. Smondyrev, S.G. Bardenhagen, P. McMurtry, G.A. Voth. Calculating the bulk modulus for a lipid bilayer with nonequilibrium molecular dynamics simulation. *Biophys. J.*, **82**, 1226 (2002).

[8] A.K. Sum, R. Faller, J.J. de Pablo. Molecular simulation study of phospholipid bilayers and insights of the interactions with disaccharides. *Biophys. J.*, **85**, 2030 (2003).

[9] C.S. Pereira, R.D. Lins, I. Chandrasekhar, L.C. Freitas, P.H. Hünenberger. Interaction of the disaccharide trehalose with a phospholipid bilayer: a molecular dynamics study. *Biophys. J.*, **85**, 2273 (2004).

[10] M.A. Villarreal, S.B. Díaz, E.A. Disalvo, G.G. Montich. Molecular dynamics simulation study of the interaction of trehalose with lipid membranes. *Langmuir*, **20**, 7844 (2004).

[11] J.F. Nagle, S. Tristram-Nagle. The Structure of lipid bilayers. *Biochem. Biphys. Acta. Rev. of Biomembranes*, **1469**, 159 (2000).

[12] B.R. Brooks, R.E. Bruccoleri, B.D. Olafson, D.J. States, S. Swaminathan, M. Karplus. CHARMM: a program for macromolecular energy, minimization, and dynamics calculations. *J. Comput. Chem.*, **4**, 187 (1983).

[13] J.B. Klauda, B.R. Brooks, A.D. MacKerell Jr, R.M. Venable, R.W. Pastor. An *ab initio* study on the torsional surface of alkanes and its effect on molecular simulations of alkanes and a DPPC bilayer. *J. Phys. Chem. B*, **109**, 5300 (2005).

[14] M. Kuttel, J.W. Brady, K.J. Naidoo. Carbohydrate solution simulations: producing a force field with experimentally consistent primary alcohol rotational frequencies and populations. *J. Comput. Chem.*, **23**, 1236 (2002).

[15] W.L. Jorgensen, J. Chandrasekhar, J.D. Madura, R.W. Impey, M.L. Klein. Comparison of simple potential functions for simulating liquid water. *J. Chem. Phys.*, **79**, 926 (1983).

[16] S.R. Durell, B.R. Brooks, A. Ben-Naim. Solvent-induced forces between 2 hydrophillic groups. *J. Phys. Chem.*, **98**, 2198 (1994).

[17] W.G. Hoover. Canonical dynamics: equilibrium phase-space distributions. *Phys. Rev. A*, **31**, 1695 (1985).

[18] S. Nosé, M.L. Klein. Constant pressure molecular dynamics for molecular systems. *Mol. Phys.*, **50**, 1055 (1983).

[19] U. Essmann, L. Perera, M.L. Berkowitz, T. Darden, H. Lee, L.G. Pedersen. A smooth particle mesh Ewald method. *J. Chem. Phys.*, **103**, 8577 (1995).

[20] P. Lagüe, R.W. Pastor, B.R. Brooks. Pressure-based long-range correction for Lennard-Jones interactions in molecular dynamics simulations: application to alkanes and interfaces. *J. Phys. Chem. B*, **108**, 363 (2004).

[21] Y. Zhang, S.E. Feller, B.R. Brooks, R.W. Pastor. Computer simulation of liquid/liquid interfaces. I. Theory and application to octane/water. *J. Chem. Phys.*, **103**, 10252 (1995).

[22] S.E. Feller, Y. Zhang, R.W. Pastor. Computer simulation of liquid/liquid interfaces. II. Surface tension-area dependence of a bilayer and monolayer. *J. Chem. Phys.*, **103**, 10267 (1995).

[23] S.E. Feller, R.W. Pastor. Constant surface tension simulations of lipid bilayers: the sensitivity of surface areas and compressibilities. *J. Chem. Phys.*, **111**, 1281 (1999).

[24] H.J.C. Berendsen, J.P.M. Postma, W.F. van Gunsteren, A. DiNola, J.R. Haak. Molecular dynamics with coupling to an external bath. *J. Chem. Phys.*, **81**, 3684 (1984).

[25] S.E. Feller, Y. Zhang, R.W. Pastor, B.R. Brooks. Constant pressure molecular dynamics simulation: the Langevin piston method. *J. Chem. Phys.*, **103**, 4613 (1995).

[26] M.A. Kiselev, J. Zbytovska, D. Matveev, S. Wartewig, I.V. Gapienko, J. Perez, P. Lesieur, A. Hoell, R. Neubert. Influence of trehalose on the structure of unilamellar DMPC vesicles.

Colloids and Surfaces A: Physicochem. Eng. Aspects, **256**, 1 (2005).

[27] Handbook of Chemistry and Physics. *A Ready-Reference Book of Chemical and Physical Data*, R.C. Weast (Ed.), 57 ed., CRC Press, Cleveland (1977).

[28] M.E. Elias, A.M. Elias. Trehalose + water fragile system: properties and glass transition. *J. Mol. Liquids*, **83**, 303 (1999).

[29] H. Petrache, S.E. Feller, J.F. Nagle. Determination of component volumes of lipid bilayers from simulations. *Biophys. J.*, **70**, 2237 (1997).

[30] S. Mitaku, A. Ikegami, A. Sakanishi. Ultrasonic studies of lipid bilayer. Phase transition in synthetic phosphatidylcholine liposomes. *Biophysical Chem.*, **8**, 295 (1978).

[31] E. Evans, W. Rawicz. Entropy-driven tension and binding elasticity in condensed-fluid membranes. *Phys. Rev. Lett.*, **64**, 2094 (1990).

[32] B.W. Koenig, H.H. Strey, K. Gawrisch. Membrane lateral compressibility determined by NMR and X-ray diffraction: effect of acyl chain polyunsaturation. *Biophys. J.*, **73**, 1954 (1997).

[33] W. Rawicz, K.C. Olbrich, T. McIntosh, D. Needham, E. Evans. Effect of chain length and unsaturation on elasticity of lipid bilayers. *Biophys. J.*, **79**, 328 (2000).